OPEN ACCESS Plant Protection, 10 (02) 2026. 141-157 DOI:10.33804/pp.010.02.5886

Check for updates

Available Online at EScience Press

Plant Protection

ISSN: 2617-1287 (Online), 2617-1279 (Print)

http://esciencepress.net/journals/PP

Research Article

Comparative Evaluation of Silica and Silver Nanoparticles for Alleviating Biotic Stress Caused by *Fusarium graminearum* in Wheat through Modulation of Physiological and Antioxidant Defense Mechanisms

Fazeelat Batool, Sumera Iqbal, Khajista Jabeen, Sumera Javad

Department of Botany, Lahore College for Women University, Lahore, Pakistan.

ARTICLE INFO

Article history

Received: 7th October, 2025

Revised: 1st March, 2026

Accepted: 6th March, 2026

Keywords

Silver nanoparticles (AgNPs)

Silica nanoparticles (SiNPs)

Fusarium graminearum

Triticum aestivum L.

Antioxidant defense system

ABSTRACT

Fungal pathogens pose a serious threat to wheat productivity by impairing plant water relations, membrane integrity, and metabolic functions. Recent advances in nanotechnology have highlighted the potential of nanoparticles as priming agents to enhance plant tolerance against biotic stresses. Therefore, this study evaluated the efficacy of silver nanoparticles (AgNPs) and silica nanoparticles (SiNPs) in modulating physiological and biochemical responses of wheat under fungal stress. Fungal infection significantly reduced relative water content (RWC), membrane stability index (MSI), protein content, osmotic potential, and photosynthetic pigments, while increasing soluble sugars, proline accumulation, and antioxidant enzyme activities. However, nanoparticle priming markedly alleviated these adverse effects in a concentration-dependent manner. AgNPs at 50-75 mg L^{-1} and SiNPs at 50-100 mg L^{-1} significantly improved RWC and MSI under stress. Protein content was maximized at 75 mg L^{-1} AgNPs and 100 mg L^{-1} SiNPs. Both nanoparticles further enhanced soluble sugar accumulation and reduced osmotic potential, indicating improved osmotic adjustment. Chlorophyll and carotenoid contents were notably enhanced, particularly with 75 mg L^{-1} AgNPs and 100 mg L^{-1} SiNPs. Although proline levels increased under stress, nanoparticle treatments generally reduced its accumulation compared to untreated stressed plants. Furthermore, higher concentrations of both nanoparticles significantly stimulated antioxidant enzyme activities (SOD, POD, and CAT), strengthening the plant defense system. In conclusion, AgNPs and SiNPs alleviate fungal stress in wheat by enhancing physiological stability and biochemical defenses, with 75 mg L^{-1} AgNPs and 100 mg L^{-1} SiNPs identified as optimal concentrations for improving stress tolerance and supporting sustainable crop protection.

Corresponding Author: Sumera Iqbal

Email: sumeraiqbal2@yahoo.com

Introduction

Wheat (*Triticum aestivum* L.) is one of the most important and widely cultivated cereal crops worldwide (Goyal and Prasad, 2010). However, wheat production is severely constrained by various biotic stresses, particularly fungal diseases caused by *Fusarium* species. Members of the genus *Fusarium* are cosmopolitan, hemibiotrophic fungal pathogens that infect wheat under favorable environmental conditions, especially high temperatures and high humidity (Hu et al., 2022). Agronomic practices such as minimum

tillage can further promote disease development because *Fusarium* spp. are soil-borne pathogens capable of surviving on infected crop residues. Moreover, ongoing climate change, characterized by increasing temperatures and altered precipitation patterns, is expected to accelerate the spread and severity of *Fusarium*-associated diseases (Schoneberge et al., 2019).

The development and cultivation of resistant cultivars represent one of the most effective strategies for managing fungal diseases in wheat. However, excessive reliance on a limited number of cultivars can lead to genetic uniformity, thereby reducing genetic diversity and increasing crop vulnerability to pathogens, pests, and environmental stresses (McDonald and Linde, 2002). Although fungicides remain widely used for controlling fungal diseases, their extensive application raises concerns regarding environmental contamination, pathogen resistance, and potential risks to human health (Hovmøller et al., 2016).

In recent years, nanotechnology has emerged as a promising alternative or complementary approach to conventional disease management strategies, including chemical, biological, and cultural control methods. Nanoparticles offer several advantages, such as enhanced antimicrobial efficacy, reduced chemical input, and lower ecological toxicity (Nazir et al., 2019; Sultana et al., 2019; Shahbaz et al., 2023). Among the various nanoparticle synthesis methods, green synthesis has gained considerable attention because it is simple, cost-effective, environmentally friendly, and capable of producing stable nanoparticles with minimal toxic byproducts, making it suitable for large-scale production (Malhotra and Alghuthaymi, 2022; Jamil et al., 2025; Hussain et al., 2026; Mehak et al., 2026).

Silver nanoparticles (AgNPs) and silicon nanoparticles (SiNPs) have been reported to enhance plant resistance against several pathogens, including *Fusarium* species, by strengthening plant cell walls and activating plant defense responses (Sabir et al., 2022; Shuja et al., 2023). Nevertheless, studies exploring the potential of these nanoparticles for the management of soil-borne diseases, particularly Fusarium head blight (FHB) caused by *Fusarium graminearum*, remain limited. Furthermore, the physiological and biochemical mechanisms underlying nanoparticle-mediated disease suppression require further investigation.

Therefore, the present study aimed to evaluate the comparative effects of biosynthesized silicon nanoparticles and silver nanoparticles on the morphophysiological and biochemical responses of wheat plants under *F. graminearum* infection.

Materials and Methods

The experiment was conducted during the 2022 wheat growing season. Seeds of wheat cultivar 'Inqilab-91' and the fungal isolate were obtained from the National Agricultural Research Center (NARC), Islamabad.

Procedure

Pot experiment (*in vivo* assay)

The experiment was carried out in plastic pots (30 cm diameter). Each pot was filled with 10 kg of soil. Wheat seeds were surface-sterilized using a 5% sodium hypochlorite solution, rinsed thoroughly with distilled water, and sown at a rate of 20 seeds per pot. The pots were irrigated as required. Seed priming was performed prior to sowing using silver and silica nanoparticles at concentrations of 25, 50, 75, 100, and 125 mg L^{-1}. A control treatment without fungal inoculation and nanoparticle application was also maintained.

Fungal stress was induced using *Fusarium graminearum* through a seed-soaking inoculation method. Each treatment was replicated three times, and the pots were arranged in a completely randomized design (CRD). The detail of treatments has been given in Table 1.

Table 1. Details of treatments.

Sr. No.	Treatments	Treatment Details
1	Control	Without fungus and without NPs.
2	T1	25 mg/L AgNPs
3	T2	50 mg/L AgNPs
4	T3	75 mg/L AgNPs
5	T4	100 mg/L AgNPs
6	T5	125 mg/L AgNPs
7	T6	25 mg/L SiNPs
8	T7	50 mg/L SiNPs
9	T8	75 mg/L SiNPs
10	T9	100 mg/L SiNPs
11	T10	125 mg/L SiNPs
12	F.S	Fungal stress
13	T1 + F.S	25 mg/L AgNPs/L + Fungal stress
14	T2 + F.S	50 mg/L AgNPs + Fungal stress
15	T3 + F.S	75 mg/L + Fungal stress
16	T4 + F.S	100 mg/L AgNPs + Fungal stress
17	T5 + F.S	125 mg/L AgNPs + Fungal stress
18	T6 + F.S	25 mg/L SiNPs + Fungal stress
19	T7 + F.S	50 mg/L SiNPs + Fungal stress
20	T8 + F.S	75 mg/L SiNPs + Fungal stress
21	T9 + F.S	100 mg/L SiNPs + Fungal stress
22	T10 + F.S	125 mg/L SiNPs + Fungal stress

After 10 days of germination, seedlings were thinned to maintain uniform plant density. Plants were irrigated as required. Sampling was conducted at the reproductive stage. After recording fresh weight, the samples were stored in a refrigerator for further analysis. The following parameters were determined.

Physicochemical properties of soil used for the pot experiment

Soil electrical conductivity (EC) was measured using a Milwaukee SM302 EC meter (Rayment and Higginson, 1992). Soil pH was determined from the soil extract using a Milwaukee SM101 pH meter (McLean, 1982). Soil texture was determined following the method described by Brady (1990). Briefly, a 100 g soil sample was mixed with water and stirred for 10 min. Subsequently, 20 ml of saturated sodium oxalate solution was added, and the mixture was shaken for an additional 5 min to disperse soil aggregates. The suspension was then transferred to a 1000 ml measuring cylinder, and the temperature was recorded. Hydrometer readings were taken at specified intervals, including an initial reading and a final reading after 4 h. The percentages of sand, silt, and clay were calculated based on hydrometer readings, and soil texture was determined using the textural triangle. Soil organic matter content was estimated following the method of Estefan et al. (2013). The physicochemical characteristics of the soil used for the pot experiment are presented in Table 2.

Table 2. Physicochemical characteristics of the soil used in the pot experiment.

Sr. No.	Physiochemical properties	Test results
1	Electrical conductivity	235µS/cm
2	pH	6.8
3	Soil texture	clay loam
4	Soil organic matter	40

Physiological and biochemical parameters of plants

Relative water content

Relative water content (RWC) was determined using the fresh weight (FW), turgid weight (TW), and dry weight (DW) of leaf samples from each replicate, following the method of Barrs and Weatherley (1962). RWC was calculated using the following formula:

$$\text{RWC } \% = \frac{\text{FW} - \text{DW}}{\text{TW} - \text{DW}} \times 100$$

Membrane stability index

The membrane stability index (MSI) was determined according to the method of Premchandra (1990), later modified by Sairam (1994). Leaf samples (0.1 g) were washed thoroughly and incubated in 10 ml of distilled water at 40°C for 30 min in a water bath. Electrical conductivity (C_1) was recorded. The samples were then heated at 100°C for 10 min, and final conductivity (C_2) was measured. MSI was calculated as:

$$\text{MSI} = 1 - \frac{\text{C1}}{\text{C2}} \times 100$$

Total soluble protein content

Total soluble protein content was estimated using the method of Lowry et al. (1951). Plant tissue (0.1 g) was homogenized in sodium phosphate buffer and centrifuged. The supernatant was reacted with appropriate reagents, and absorbance was measured at 650 nm. Protein concentration was determined using bovine serum albumin (BSA) as a standard.

Total soluble sugars

Total soluble sugars were determined following the method of Dubois et al. (1956). Leaf samples (0.5 g) were homogenized in distilled water and filtered. The filtrate was treated with 5% phenol, followed by the addition of concentrated sulfuric acid. After incubation at room temperature, absorbance was measured at 420 nm using a spectrophotometer, and sugar content was calculated from a standard glucose curve.

Osmotic potential

Leaf sap osmotic potential was measured using a vapor pressure osmometer, following the method of Capell and Doerffling (1993). Sap extracted from frozen-thawed leaf samples was analyzed, and osmolality (mmol kg^{-1}) was converted to osmotic potential (MPa) using the following equation:

Osmotic potential (MPa) = − (osmolality × 0.008314 × T)

Where T is the absolute temperature in Kelvin.

Chlorophyll contents

For chlorophyll estimation, fresh leaf samples (0.1 g) were homogenized using a mortar and pestle in 80% acetone and filtered. Absorbance was recorded at 663, 645, and 470 nm using a spectrophotometer. Chlorophyll a, chlorophyll b, and total chlorophyll contents were calculated using the equations described by Arnon (1949):

Chlorophyll a = $12.21(A_{663}) - 2.81(A_{645})$

Chlorophyll b = $20.13(A_{645}) - 5.03(A_{663})$

Total chlorophyll = $20.2(A_{645}) + 8.02(A_{663})$

Carotenoid content was determined according to Lichtenthaler and Wellburn (1983) using the following formula:

$$\text{Carotenoids} = \frac{[1000(A_{470}) - 2.27(\text{Chl a}) - 81.4(\text{Chl b})]}{227}$$

The chlorophyll a/b ratio was calculated by dividing chlorophyll a by chlorophyll b. Pigment concentration was expressed on a fresh weight basis using the formula:

$$\text{Pigment content} = \frac{C \times V}{1000 \times W}$$

Where C is pigment concentration, V is the volume of extract, and W is the fresh weight of the leaf sample.

Proline content

Proline content was estimated following the method of Bates et al. (1973). Frozen leaf samples were extracted with sulfosalicylic acid and centrifuged. The supernatant was reacted with acid ninhydrin and glacial acetic acid, and then heated in a boiling water bath. The resulting chromophore was extracted with toluene, and absorbance was measured at 520 nm. Proline concentration was calculated using a standard curve.

Antioxidant enzyme activities

Enzymes were extracted by homogenizing 0.5 g of fresh leaf tissue in an ice bath using a mortar and pestle. The homogenate was prepared in 5 ml of phosphate buffer and subsequently centrifuged at 13,000 rpm for 20 min at 4°C. The supernatant was collected and used for enzymatic assays.

Superoxide dismutase (SOD) activity

SOD activity was determined following the method of Beauchamp and Fridovich (1971), based on the inhibition of the photochemical reduction of nitroblue tetrazolium (NBT). The reaction mixture consisted of methionine, NBT, Triton X-100, phosphate buffer, enzyme extract, and riboflavin. The reaction was initiated by exposing the mixture to UV light for 15 min. Absorbance was recorded at 560 nm using a spectrophotometer. SOD activity was expressed per 100 mg fresh weight using the following formula:

$$\text{SOD activity (IU) per 100 mg F. wt.} = \frac{\text{Absorbance} \times 1050}{W \times 100}$$

Peroxidase (POD) activity

Peroxidase activity was assayed by mixing the enzyme extract with phosphate buffer (pH 7.0), p-phenylenediamine, and hydrogen peroxide. The reaction was monitored for 3 min using a dual-beam spectrophotometer at 485 nm. One unit of peroxidase activity was defined as a unit change in optical density per minute at 485 nm (Vetter et al., 1958; Gorin and Heidema, 1976). Enzyme activity was calculated using a standard calibration curve and expressed as:

POD activity = ΔA485/ mg protein

Catalase (CAT) activity

Catalase activity was determined by mixing 0.2 ml hydrogen peroxide with 0.2 ml enzyme extract and 2 ml potassium phosphate buffer (K_2PO_4, pH 7.2). The reaction was allowed to proceed for 5 min and then terminated by adding 2 ml of titanium reagent, resulting in the formation of a yellow-colored complex. The mixture was centrifuged at 600 rpm for 10 min, and the absorbance of the supernatant was measured at 410 nm. Catalase activity was calculated according to Teranishi et al. (1974) using the following expression:

Catalase activity = ΔA410 /mg protein

Where ΔA_{410} represents the change in absorbance at 410 nm immediately after mixing the enzyme extract with the substrate.

Data analysis

The data were subjected to one-way analysis of variance (ANOVA) to determine the significance of differences among treatments. Treatment means were considered significantly different at $P \leq 0.05$. Tukey's Honestly Significant Difference (HSD) test was used for multiple comparisons of means. All statistical analyses were performed using Statistix 8.1 software.

Results

Physiological and biochemical parameters of plants

Relative water content

In the present study, the relative water content (RWC) of wheat leaves decreased under fungal stress; however, it improved significantly ($P < 0.05$) following silver nanoparticle (AgNP) priming at 25, 50, and 75 mg L^{-1} and silica nanoparticle (SiNP) priming at 50 and 100 mg L^{-1}. In contrast, higher concentrations of AgNPs (100 and 125 mg L^{-1}), as well as the lowest (25 mg L^{-1}) and highest (125 mg L^{-1}) concentrations of SiNPs, exhibited no significant effect under fungal stress (Figure 1).

Membrane stability index

The membrane stability index (MSI) (Figure 2) was reduced in all treatments compared with the control. However, all concentrations of SiNPs and two concentrations of AgNPs (50 and 75 mg L^{-1}) significantly ($P < 0.05$) improved MSI under fungal stress compared with untreated diseased plants.

Protein content

Protein content (Figure 3) decreased significantly ($P < 0.05$) under biotic stress. The highest protein content was recorded in plants treated with 75 mg L^{-1} AgNPs. SiNPs also

enhanced protein content in both stressed and non-stressed plants, with the maximum effect observed at 100 mg L^{-1}.

Soluble sugar content

Soluble sugar content (Figure 4) increased under biotic stress. Both AgNPs and SiNPs further elevated sugar levels in stressed plants, particularly at higher concentrations (≥ 75 mg L^{-1}).

Osmotic potential

Fungal stress significantly ($P < 0.05$) reduced the osmotic potential of leaves (Figure 5). Application of both nanoparticles further decreased osmotic potential in both stressed and non-stressed plants in a concentration-dependent manner.

Chlorophyll contents

Fungal stress significantly reduced chlorophyll a, chlorophyll b, total chlorophyll, carotenoids, and the chlorophyll a/b ratio compared with non-stressed plants (Figure 6, 7, 8, 9 and 10). Plants treated with 75 mg L^{-1} AgNPs exhibited the highest pigment contents, whereas other AgNP concentrations showed either no significant effect or a reduction in these parameters. In contrast, SiNPs generally enhanced chlorophyll a, chlorophyll b, total chlorophyll, carotenoids, and the chlorophyll a/b ratio, except at 25 mg L^{-1}, which showed no significant effect. The highest values for all these parameters were observed in plants treated with 100 mg L^{-1} SiNPs under both stressed and non-stressed conditions.

Proline content

Proline content (Figure 11) was significantly higher in diseased plants compared with the control, irrespective of nanoparticle treatment. However, AgNPs at 25, 100, and 125 mg L^{-1} and all concentrations of SiNPs reduced proline accumulation compared with stress alone.

Antioxidant enzyme activities

The activities of antioxidant enzymes, superoxide dismutase (SOD), peroxidase (POD), and catalase (CAT), were significantly increased under stress conditions (Figure 12, 13 and 14). The lowest concentration (25 mg L^{-1}) of both nanoparticles had no significant effect on enzyme activities, whereas higher concentrations significantly enhanced enzyme activity under both control and stressed conditions.

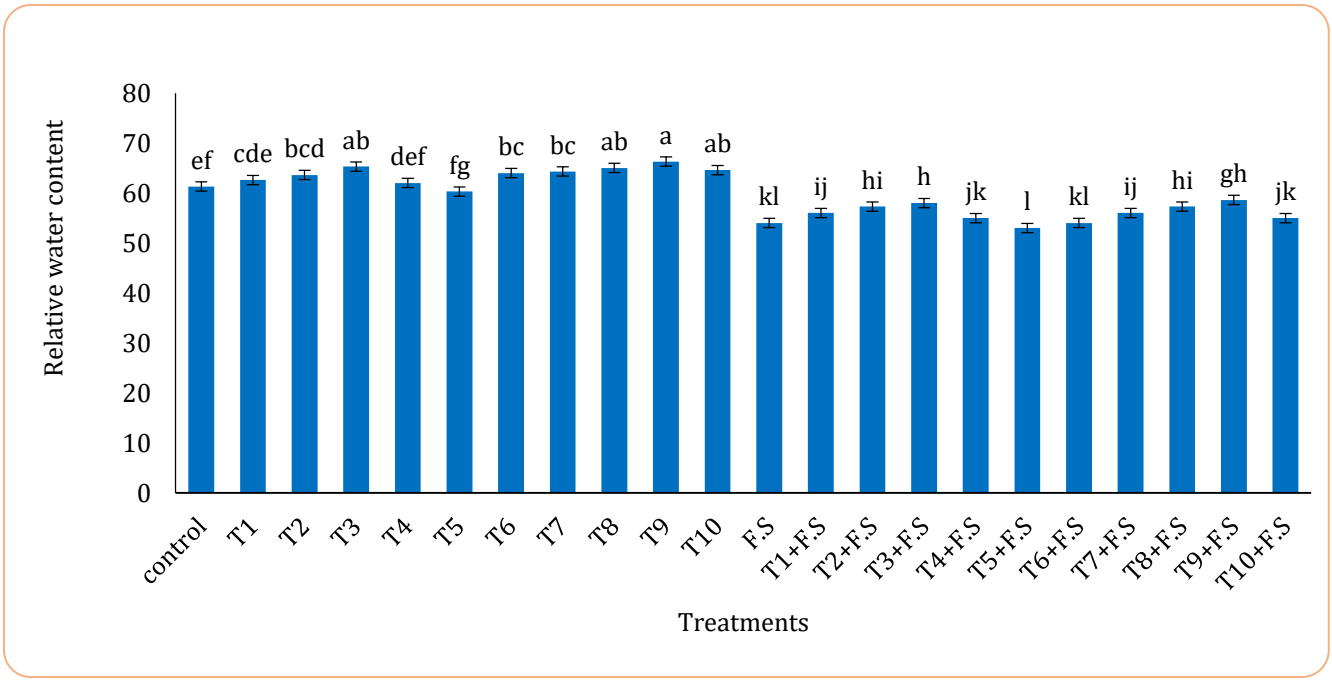

Figure 1. Effect of AgNPs and SiNPs on RWC of *T. aestivum* leaves under fungal stress.

C = control, T1 = 25mg/L AgNPs, T2 = 50mg/L AgNPs, T3 = 75mg/L AgNPs, T4 = 100mg/L AgNPs, T5 = 125mg/L AgNPs, T6 = 25mg/L SiNPs, T7 = 50mg/L SiNPs, T8 = 75mg/L SiNPs, T9 = 100mg/L SiNPs, T10 = 125mg/L SiNPs, F.S = Fungal stress, T1 + F.S = 25mg/L AgNPs/L + Fungal stress, T2 + F.S = 50mg/L AgNPs + Fungal stress, T3 + F.S = 75mg/L + Fungal stress, T4 + F.S = 100mg/L AgNPs + Fungal stress, T5 + F.S = 125mg/L AgNPs + Fungal stress, T6 + F.S = 25mg/L SiNPs + Fungal stress, T7 + F.S = 50mg/L SiNPs + Fungal stress, T8 + F.S = 75mg/L SiNPs + Fungal stress, T9 + F.S = 100mg/L SiNPs + Fungal stress, T10 = 125mg/L SiNPs + Fungal stress. Bars sharing the same letter are not significantly different at $P < 0.05$.

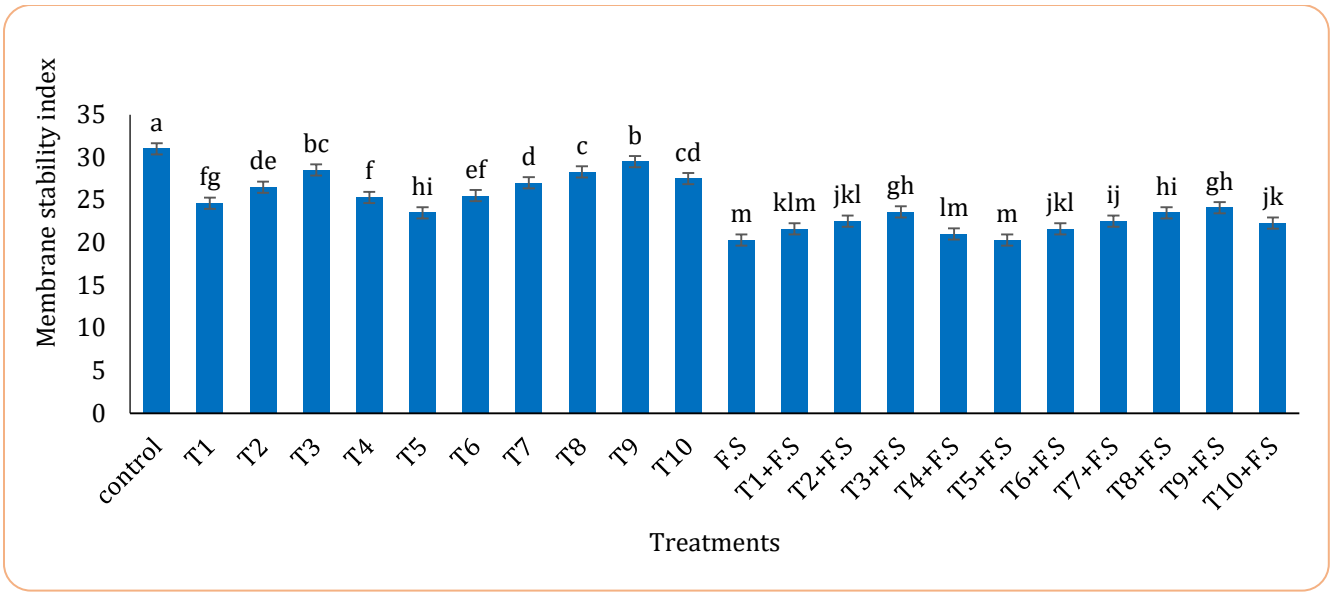

Figure 2. Effect of AgNPs and SiNPs on MSI of *T. aestivum* leaves under fungal stress.
C = control, T1 = 25mg/L AgNPs, T2 = 50mg/L AgNPs, T3 = 75mg/L AgNPs, T4 = 100mg/L AgNPs, T5 = 125mg/L AgNPs, T6 = 25mg/L SiNPs, T7 = 50mg/L SiNPs, T8 = 75mg/L SiNPs, T9 = 100mg/L SiNPs, T10 = 125mg/L SiNPs, F.S = Fungal stress, T1 + F.S = 25mg/L AgNPs/L + Fungal stress, T2 + F.S = 50mg/L AgNPs + Fungal stress, T3 + F.S = 75mg/L + Fungal stress, T4 + F.S = 100mg/L AgNPs + Fungal stress, T5 + F.S = 125mg/L AgNPs + Fungal stress, T6 + F.S = 25mg/L SiNPs + Fungal stress, T7 + F.S = 50mg/L SiNPs + Fungal stress, T8 + F.S = 75mg/L SiNPs + Fungal stress, T9 + F.S = 100mg/L SiNPs + Fungal stress, T10 = 125mg/L SiNPs + Fungal stress. Bars sharing the same letter are not significantly different at $P < 0.05$.

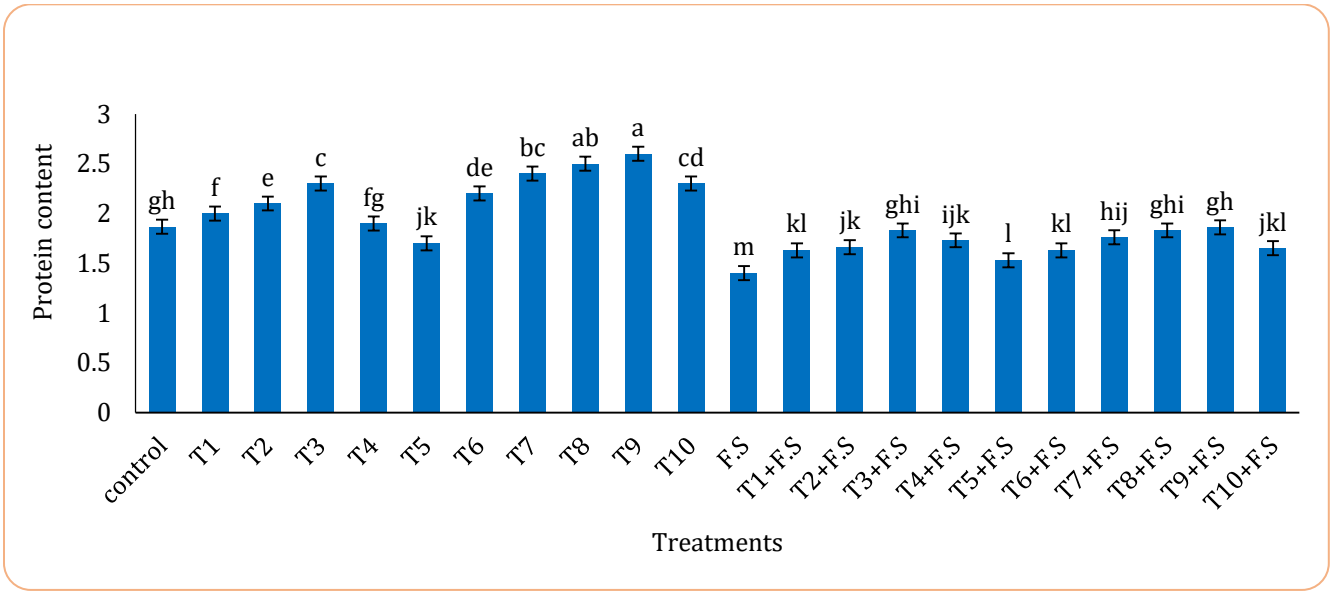

Figure 3. Effect of AgNPs and SiNPs on protein content of *T. aestivum* leaves under fungal stress.
C = control, T1 = 25mg/L AgNPs, T2 = 50mg/L AgNPs, T3 = 75mg/L AgNPs, T4 = 100mg/L AgNPs, T5 = 125mg/L AgNPs, T6 = 25mg/L SiNPs, T7 = 50mg/L SiNPs, T8 = 75mg/L SiNPs, T9 = 100mg/L SiNPs, T10 = 125mg/L SiNPs, F.S = Fungal stress, T1 + F.S = 25mg/L AgNPs/L + Fungal stress, T2 + F.S = 50mg/L AgNPs + Fungal stress, T3 + F.S = 75mg/L + Fungal stress, T4 + F.S = 100mg/L AgNPs + Fungal stress, T5 + F.S = 125mg/L AgNPs + Fungal stress, T6 + F.S = 25mg/L SiNPs + Fungal stress, T7 + F.S = 50mg/L SiNPs + Fungal stress, T8 + F.S = 75mg/L SiNPs + Fungal stress, T9 + F.S = 100mg/L SiNPs + Fungal stress, T10 = 125mg/L SiNPs + Fungal stress. Bars sharing the same letter are not significantly different at $P < 0.05$.

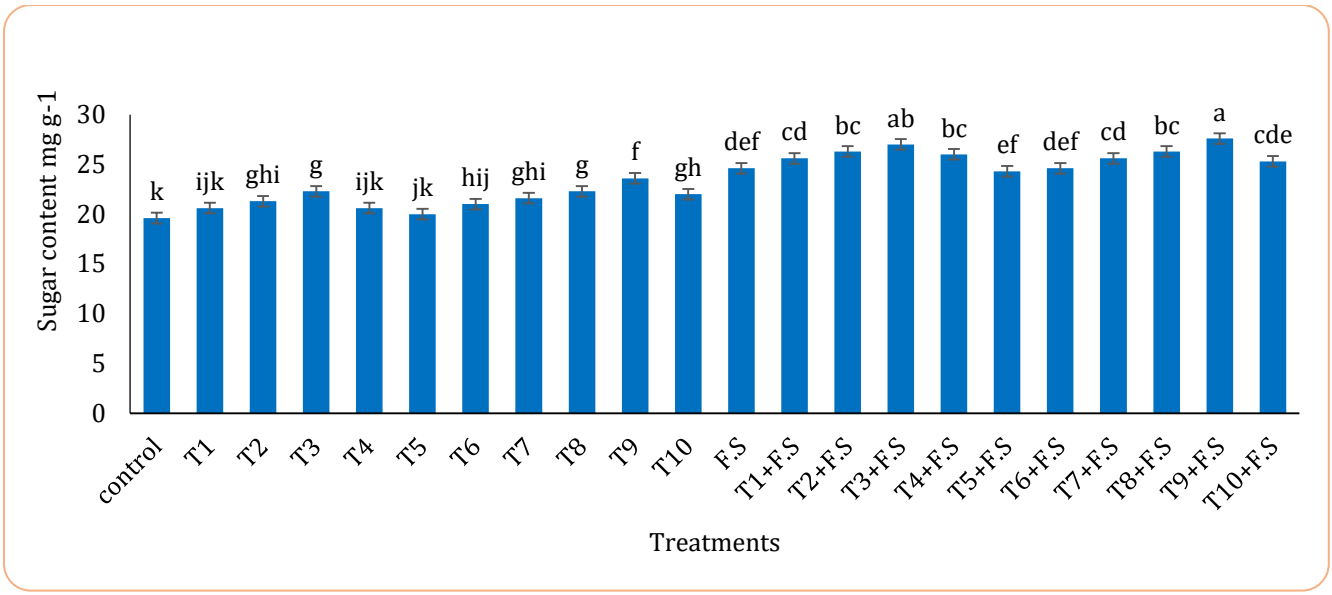

Figure 4. Effect of AgNPs and SiNPs on sugar content of *T. aestivum* leaves under fungal stress.
C = control, T1 = 25mg/L AgNPs, T2 = 50mg/L AgNPs, T3 = 75mg/L AgNPs, T4 = 100mg/L AgNPs, T5 = 125mg/L AgNPs, T6 = 25mg/L SiNPs, T7 = 50mg/L SiNPs, T8 = 75mg/L SiNPs, T9 = 100mg/L SiNPs, T10 = 125mg/L SiNPs, F.S = Fungal stress, T1 + F.S = 25mg/L AgNPs/L + Fungal stress, T2 + F.S = 50mg/L AgNPs + Fungal stress, T3 + F.S = 75mg/L + Fungal stress, T4 + F.S = 100mg/L AgNPs + Fungal stress, T5 + F.S = 125mg/L AgNPs + Fungal stress, T6 + F.S = 25mg/L SiNPs + Fungal stress, T7 + F.S = 50mg/L SiNPs + Fungal stress, T8 + F.S = 75mg/L SiNPs + Fungal stress, T9 + F.S = 100mg/L SiNPs + Fungal stress, T10 = 125mg/L SiNPs + Fungal stress. Bars sharing the same letter are not significantly different at $P < 0.05$.

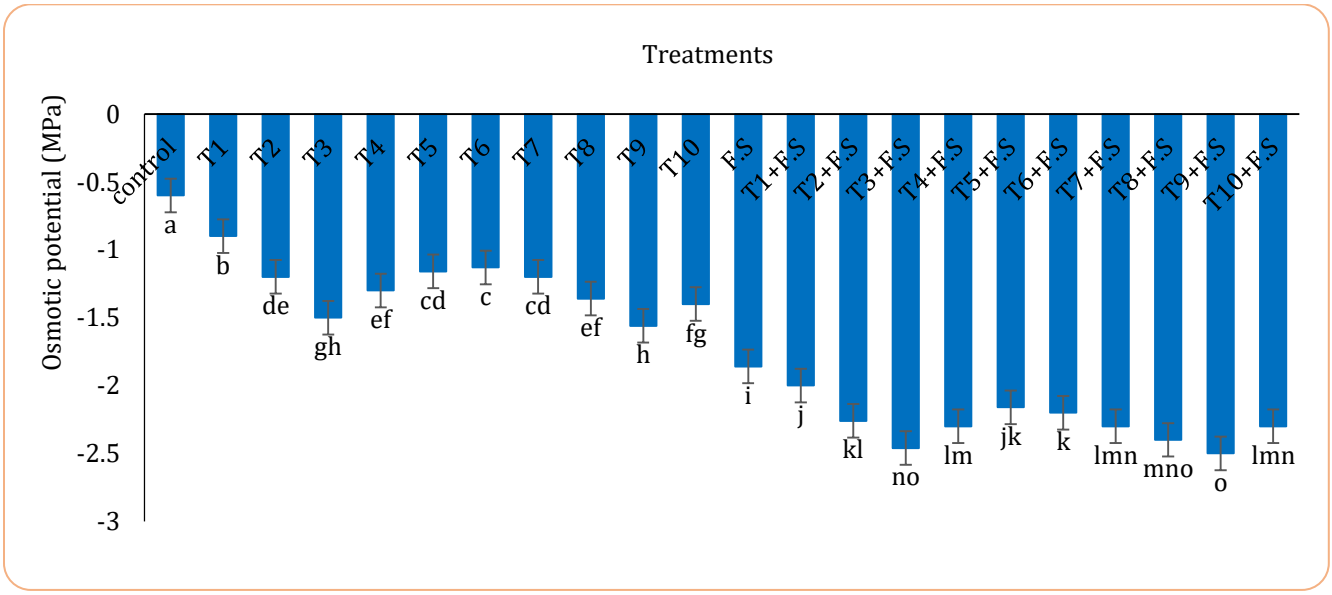

Figure 5. Effect of AgNPs and SiNPs on osmotic otential of *T. aestivum* leaves under fungal stress.
C = control, T1 = 25mg/L AgNPs, T2 = 50mg/L AgNPs, T3 = 75mg/L AgNPs, T4 = 100mg/L AgNPs, T5 = 125mg/L AgNPs, T6 = 25mg/L SiNPs, T7 = 50mg/L SiNPs, T8 = 75mg/L SiNPs, T9 = 100mg/L SiNPs, T10 = 125mg/L SiNPs, F.S = Fungal stress, T1 + F.S = 25mg/L AgNPs/L + Fungal stress, T2 + F.S = 50mg/L AgNPs + Fungal stress, T3 + F.S = 75mg/L + Fungal stress, T4 + F.S = 100mg/L AgNPs + Fungal stress, T5 + F.S = 125mg/L AgNPs + Fungal stress, T6 + F.S = 25mg/L SiNPs + Fungal stress, T7 + F.S = 50mg/L SiNPs + Fungal stress, T8 + F.S = 75mg/L SiNPs + Fungal stress, T9 + F.S = 100mg/L SiNPs + Fungal stress, T10 = 125mg/L SiNPs + Fungal stress. Bars sharing the same letter are not significantly different at $P < 0.05$.

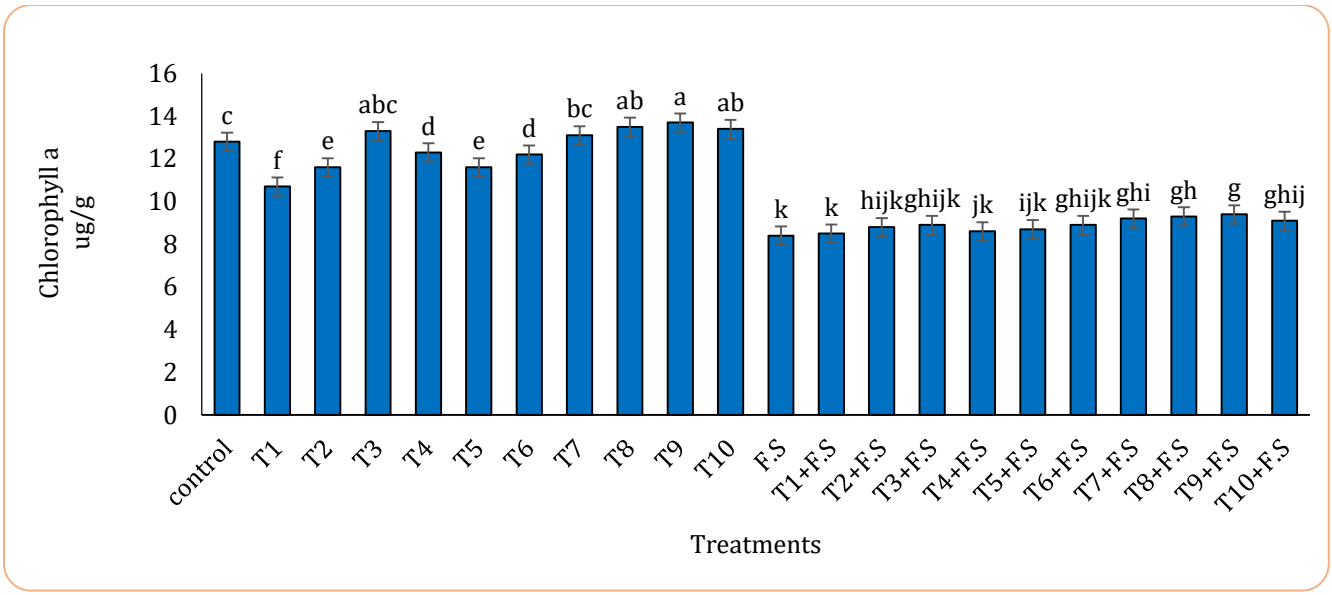

Figure 6. Effect of AgNPs and SiNPs on chlorophyll a content of *T. aestivum* leaves under fungal stress.
C = control, T1 = 25mg/L AgNPs, T2 = 50mg/L AgNPs, T3 = 75mg/L AgNPs, T4 = 100mg/L AgNPs, T5 = 125mg/L AgNPs, T6 = 25mg/L SiNPs, T7 = 50mg/L SiNPs, T8 = 75mg/L SiNPs, T9 = 100mg/L SiNPs, T10 = 125mg/L SiNPs, F.S = Fungal stress, T1 + F.S = 25mg/L AgNPs/L + Fungal stress, T2 + F.S = 50mg/L AgNPs + Fungal stress, T3 + F.S = 75mg/L + Fungal stress, T4 + F.S = 100mg/L AgNPs + Fungal stress, T5 + F.S = 125mg/L AgNPs + Fungal stress, T6 + F.S = 25mg/L SiNPs + Fungal stress, T7 + F.S = 50mg/L SiNPs + Fungal stress, T8 + F.S = 75mg/L SiNPs + Fungal stress, T9 + F.S = 100mg/L SiNPs + Fungal stress, T10 = 125mg/L SiNPs + Fungal stress. Bars sharing the same letter are not significantly different at $P < 0.05$.

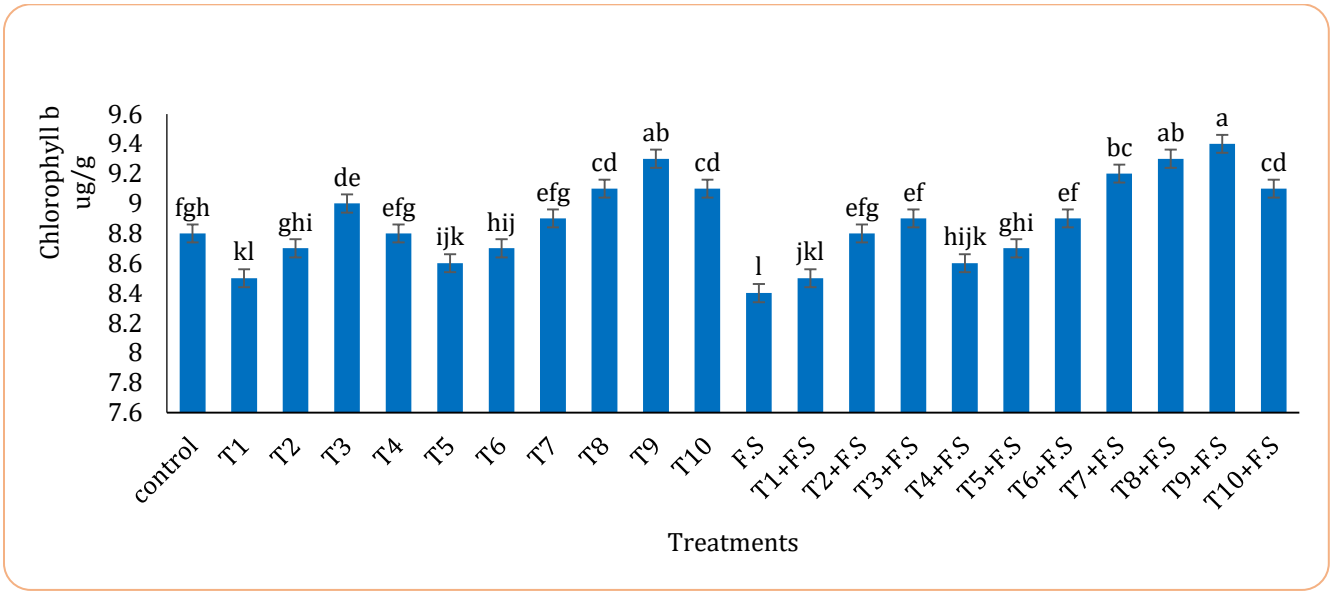

Figure 7. Effect of AgNPs and SiNPs on chlorophyll b content of *T. aestivum* leaves under fungal stress.
C = control, T1 = 25mg/L AgNPs, T2 = 50mg/L AgNPs, T3 = 75mg/L AgNPs, T4 = 100mg/L AgNPs, T5 = 125mg/L AgNPs, T6 = 25mg/L SiNPs, T7 = 50mg/L SiNPs, T8 = 75mg/L SiNPs, T9 = 100mg/L SiNPs, T10 = 125mg/L SiNPs, F.S = Fungal stress, T1 + F.S = 25mg/L AgNPs/L + Fungal stress, T2 + F.S = 50mg/L AgNPs + Fungal stress, T3 + F.S = 75mg/L + Fungal stress, T4 + F.S = 100mg/L AgNPs + Fungal stress, T5 + F.S = 125mg/L AgNPs + Fungal stress, T6 + F.S = 25mg/L SiNPs + Fungal stress, T7 + F.S = 50mg/L SiNPs + Fungal stress, T8 + F.S = 75mg/L SiNPs + Fungal stress, T9 + F.S = 100mg/L SiNPs + Fungal stress, T10 = 125mg/L SiNPs + Fungal stress. Bars sharing the same letter are not significantly different at $P < 0.05$.

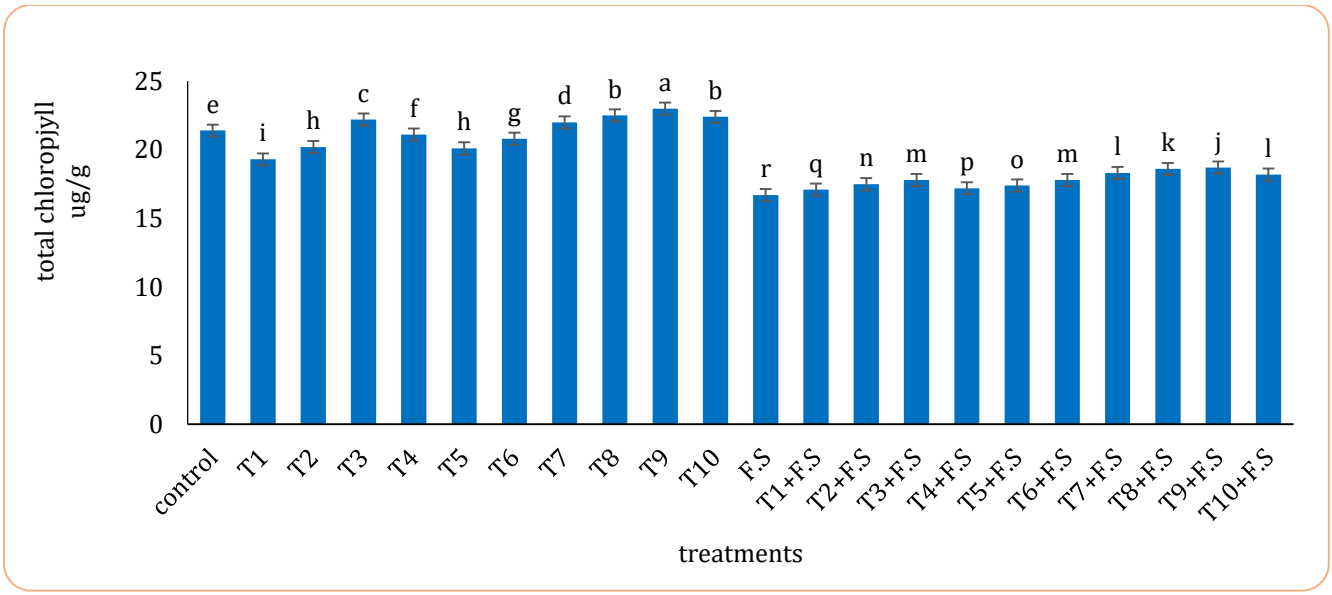

Figure 8. Effect of AgNPs and SiNPs on total chlorophyll content of *T. aestivum* leaves under fungal stress.
C = control, T1 = 25mg/L AgNPs, T2 = 50mg/L AgNPs, T3 = 75mg/L AgNPs, T4 = 100mg/L AgNPs, T5 = 125mg/L AgNPs, T6 = 25mg/L SiNPs, T7 = 50mg/L SiNPs, T8 = 75mg/L SiNPs, T9 = 100mg/L SiNPs, T10 = 125mg/L SiNPs, F.S = Fungal stress, T1 + F.S = 25mg/L AgNPs/L + Fungal stress, T2 + F.S = 50mg/L AgNPs + Fungal stress, T3 + F.S = 75mg/L + Fungal stress, T4 + F.S = 100mg/L AgNPs + Fungal stress, T5 + F.S = 125mg/L AgNPs + Fungal stress, T6 + F.S = 25mg/L SiNPs + Fungal stress, T7 + F.S = 50mg/L SiNPs + Fungal stress, T8 + F.S = 75mg/L SiNPs + Fungal stress, T9 + F.S = 100mg/L SiNPs + Fungal stress, T10 = 125mg/L SiNPs + Fungal stress. Bars sharing the same letter are not significantly different at $P < 0.05$.

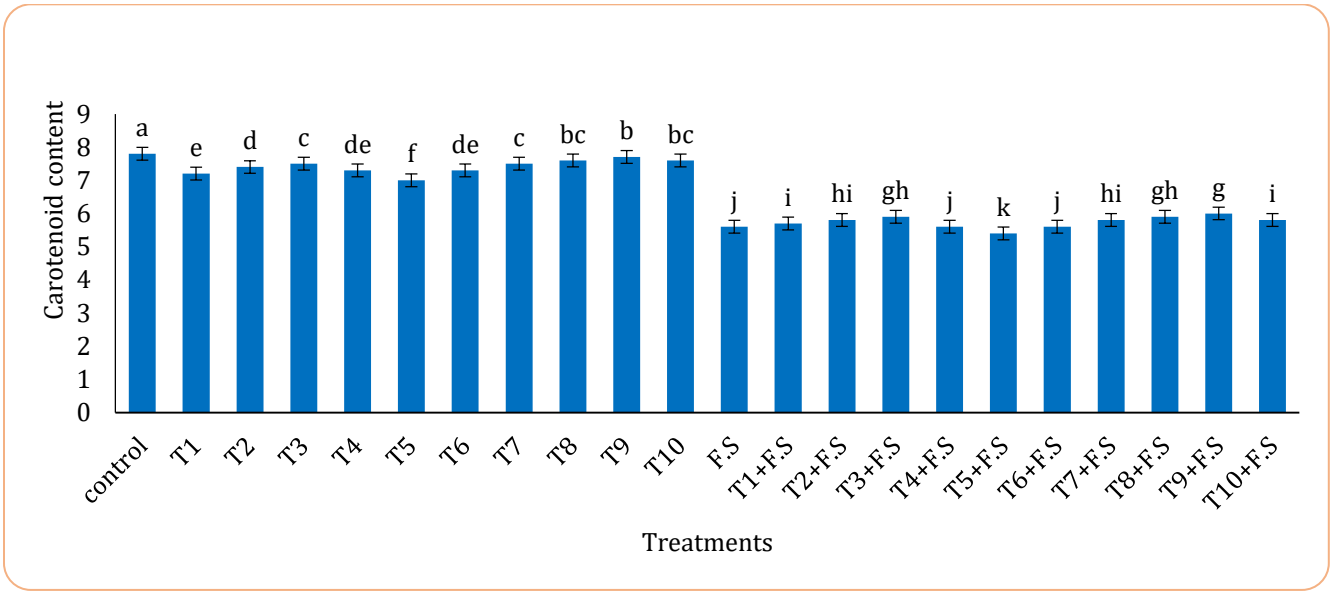

Figure 9. Effect of AgNPs and SiNPs on carotenoids of *T. aestivum* leaves under fungal stress.
C = control, T1 = 25mg/L AgNPs, T2 = 50mg/L AgNPs, T3 = 75mg/L AgNPs, T4 = 100mg/L AgNPs, T5 = 125mg/L AgNPs, T6 = 25mg/L SiNPs, T7 = 50mg/L SiNPs, T8 = 75mg/L SiNPs, T9 = 100mg/L SiNPs, T10 = 125mg/L SiNPs, F.S = Fungal stress, T1 + F.S = 25mg/L AgNPs/L + Fungal stress, T2 + F.S = 50mg/L AgNPs + Fungal stress, T3 + F.S = 75mg/L + Fungal stress, T4 + F.S = 100mg/L AgNPs + Fungal stress, T5 + F.S = 125mg/L AgNPs + Fungal stress, T6 + F.S = 25mg/L SiNPs + Fungal stress, T7 + F.S = 50mg/L SiNPs + Fungal stress, T8 + F.S = 75mg/L SiNPs + Fungal stress, T9 + F.S = 100mg/L SiNPs + Fungal stress, T10 = 125mg/L SiNPs + Fungal stress. Bars sharing the same letter are not significantly different at $P < 0.05$.

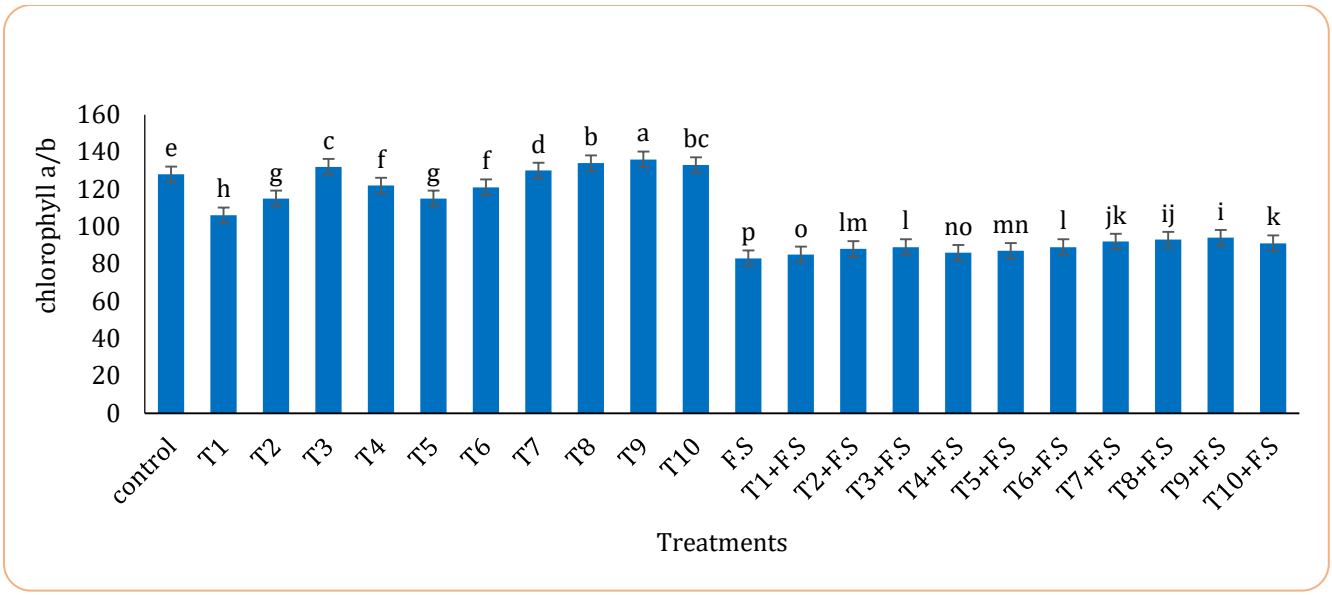

Figure 10. Effect of AgNPs and SiNPs on chlorophyll a/b content of *T. aestivum* leaves under fungal stress.
C = control, T1 = 25mg/L AgNPs, T2 = 50mg/L AgNPs, T3 = 75mg/L AgNPs, T4 = 100mg/L AgNPs, T5 = 125mg/L AgNPs, T6 = 25mg/L SiNPs, T7 = 50mg/L SiNPs, T8 = 75mg/L SiNPs, T9 = 100mg/L SiNPs, T10 = 125mg/L SiNPs, F.S = Fungal stress, T1 + F.S = 25mg/L AgNPs/L + Fungal stress, T2 + F.S = 50mg/L AgNPs + Fungal stress, T3 + F.S = 75mg/L + Fungal stress, T4 + F.S = 100mg/L AgNPs + Fungal stress, T5 + F.S = 125mg/L AgNPs + Fungal stress, T6 + F.S = 25mg/L SiNPs + Fungal stress, T7 + F.S = 50mg/L SiNPs + Fungal stress, T8 + F.S = 75mg/L SiNPs + Fungal stress, T9 + F.S = 100mg/L SiNPs + Fungal stress, T10 = 125mg/L SiNPs + Fungal stress. Bars sharing the same letter are not significantly different at $P < 0.05$.

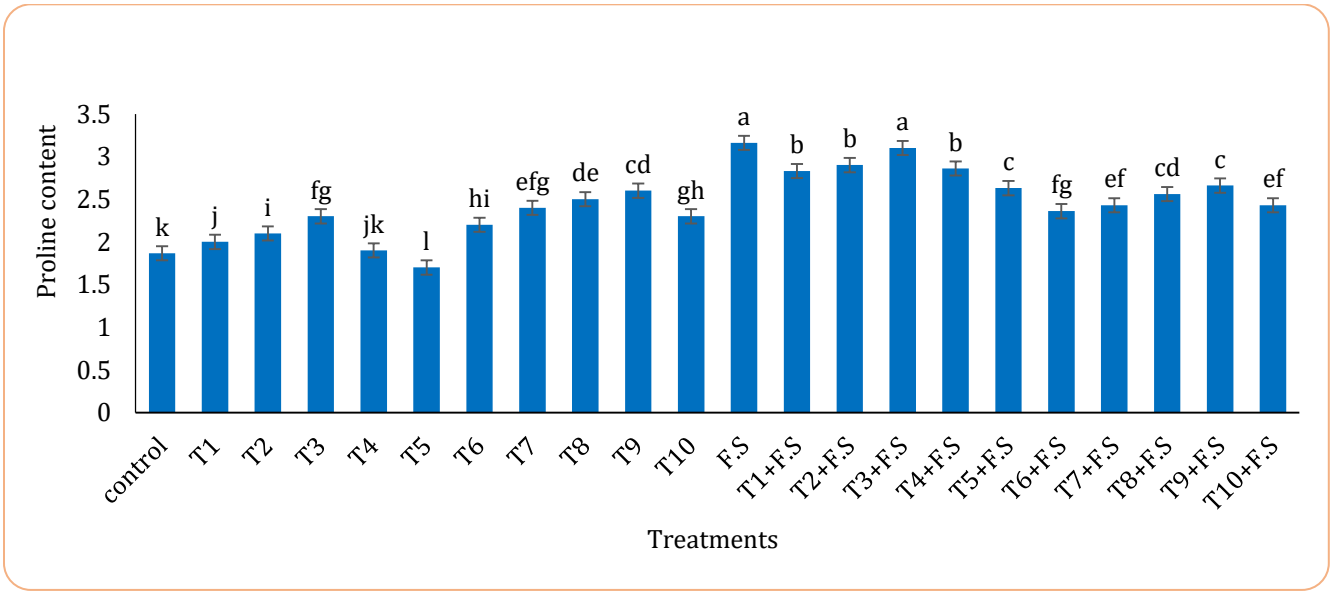

Figure 11. Effect of AgNPs and SiNPs on proline content of *T. aestivum* leaves under fungal stress.
C = control, T1 = 25mg/L AgNPs, T2 = 50mg/L AgNPs, T3 = 75mg/L AgNPs, T4 = 100mg/L AgNPs, T5 = 125mg/L AgNPs, T6 = 25mg/L SiNPs, T7 = 50mg/L SiNPs, T8 = 75mg/L SiNPs, T9 = 100mg/L SiNPs, T10 = 125mg/L SiNPs, F.S = Fungal stress, T1 + F.S = 25mg/L AgNPs/L + Fungal stress, T2 + F.S = 50mg/L AgNPs + Fungal stress, T3 + F.S = 75mg/L + Fungal stress, T4 + F.S = 100mg/L AgNPs + Fungal stress, T5 + F.S = 125mg/L AgNPs + Fungal stress, T6 + F.S = 25mg/L SiNPs + Fungal stress, T7 + F.S = 50mg/L SiNPs + Fungal stress, T8 + F.S = 75mg/L SiNPs + Fungal stress, T9 + F.S = 100mg/L SiNPs + Fungal stress, T10 = 125mg/L SiNPs + Fungal stress. Bars sharing the same letter are not significantly different at $P < 0.05$.

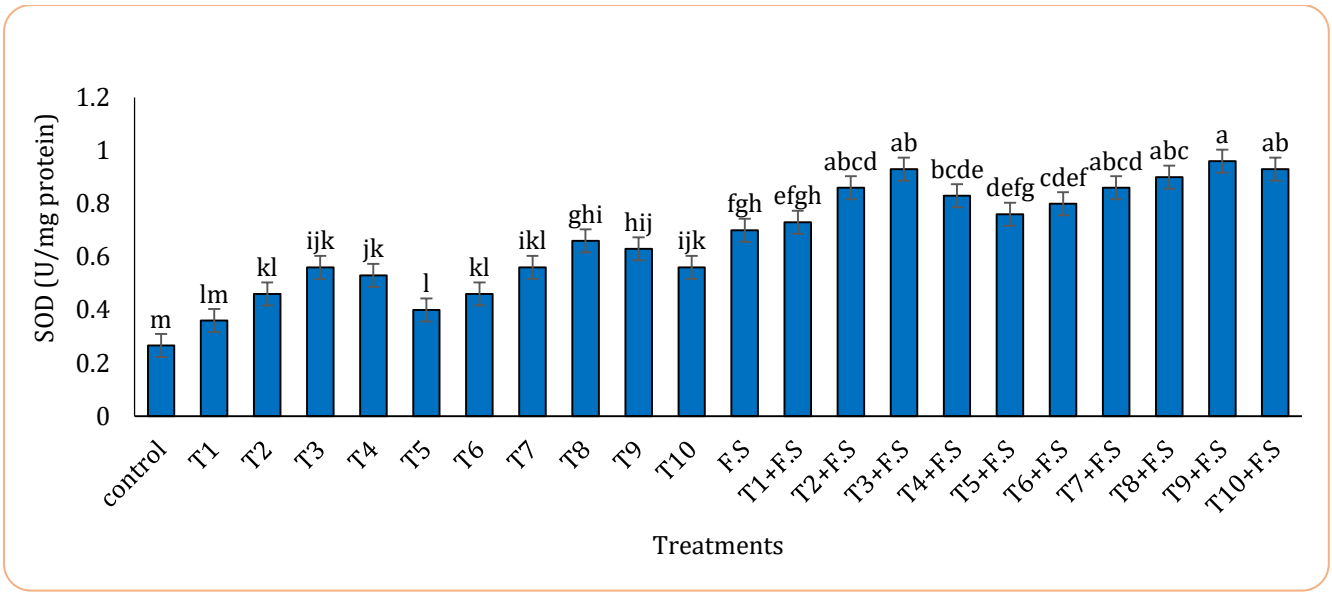

Figure 12. Effect of AgNPs and SiNPs on SOD activity of *T. aestivum* leaves under fungal stress.
C = control, T1 = 25mg/L AgNPs, T2 = 50mg/L AgNPs, T3 = 75mg/L AgNPs, T4 = 100mg/L AgNPs, T5 = 125mg/L AgNPs, T6 = 25mg/L SiNPs, T7 = 50mg/L SiNPs, T8 = 75mg/L SiNPs, T9 = 100mg/L SiNPs, T10 = 125mg/L SiNPs, F.S = Fungal stress, T1 + F.S = 25mg/L AgNPs/L + Fungal stress, T2 + F.S = 50mg/L AgNPs + Fungal stress, T3 + F.S = 75mg/L + Fungal stress, T4 + F.S = 100mg/L AgNPs + Fungal stress, T5 + F.S = 125mg/L AgNPs + Fungal stress, T6 + F.S = 25mg/L SiNPs + Fungal stress, T7 + F.S = 50mg/L SiNPs + Fungal stress, T8 + F.S = 75mg/L SiNPs + Fungal stress, T9 + F.S = 100mg/L SiNPs + Fungal stress, T10 = 125mg/L SiNPs + Fungal stress. Bars sharing the same letter are not significantly different at $P < 0.05$.

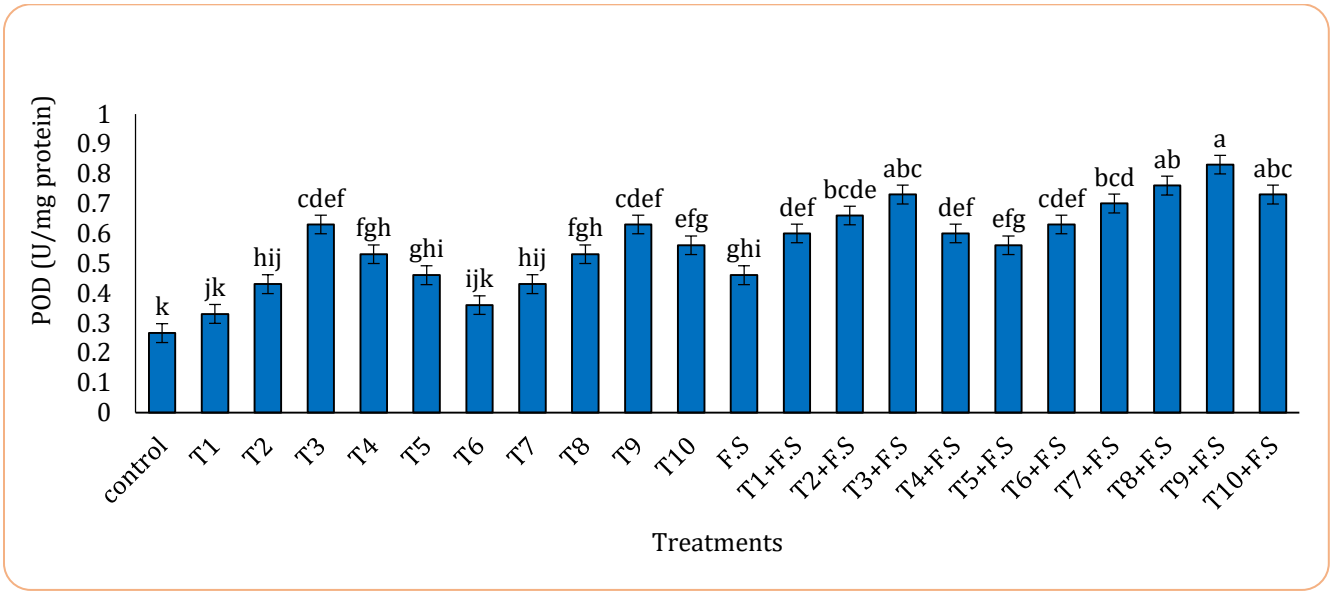

Figure 13. Effect of AgNPs and SiNPs on POD activity of *T. aestivum* leaves under fungal stress.
C = control, T1 = 25mg/L AgNPs, T2 = 50mg/L AgNPs, T3 = 75mg/L AgNPs, T4 = 100mg/L AgNPs, T5 = 125mg/L AgNPs, T6 = 25mg/L SiNPs, T7 = 50mg/L SiNPs, T8 = 75mg/L SiNPs, T9 = 100mg/L SiNPs, T10 = 125mg/L SiNPs, F.S = Fungal stress, T1 + F.S = 25mg/L AgNPs/L + Fungal stress, T2 + F.S = 50mg/L AgNPs + Fungal stress, T3 + F.S = 75mg/L + Fungal stress, T4 + F.S = 100mg/L AgNPs + Fungal stress, T5 + F.S = 125mg/L AgNPs + Fungal stress, T6 + F.S = 25mg/L SiNPs + Fungal stress, T7 + F.S = 50mg/L SiNPs + Fungal stress, T8 + F.S = 75mg/L SiNPs + Fungal stress, T9 + F.S = 100mg/L SiNPs + Fungal stress, T10 = 125mg/L SiNPs + Fungal stress. Bars sharing the same letter are not significantly different at $P < 0.05$.

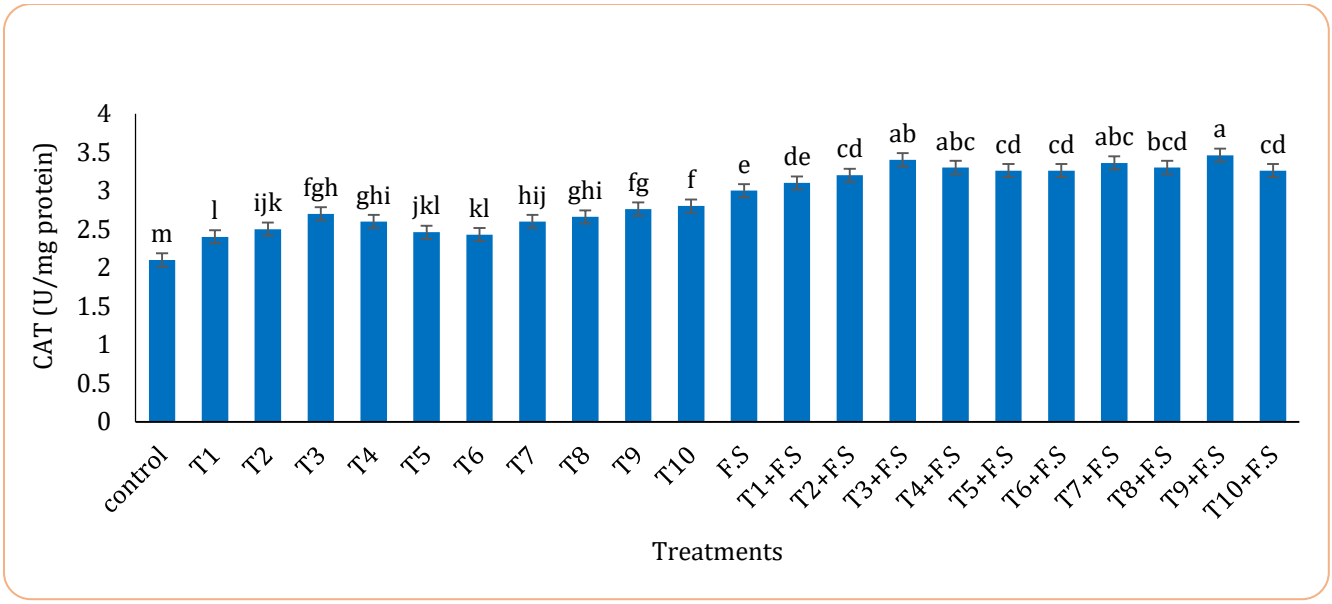

Figure 14. Effect of AgNPs and SiNPs on CAT activity of *T. aestivum* leaves under fungal stress.
C = control, T1 = 25mg/L AgNPs, T2 = 50mg/L AgNPs, T3 = 75mg/L AgNPs, T4 = 100mg/L AgNPs, T5 = 125mg/L AgNPs, T6 = 25mg/L SiNPs, T7 = 50mg/L SiNPs, T8 = 75mg/L SiNPs, T9 = 100mg/L SiNPs, T10 = 125mg/L SiNPs, F.S = Fungal stress, T1 + F.S = 25mg/L AgNPs/L + Fungal stress, T2 + F.S = 50mg/L AgNPs + Fungal stress, T3 + F.S = 75mg/L + Fungal stress, T4 + F.S = 100mg/L AgNPs + Fungal stress, T5 + F.S = 125mg/L AgNPs + Fungal stress, T6 + F.S = 25mg/L SiNPs + Fungal stress, T7 + F.S = 50mg/L SiNPs + Fungal stress, T8 + F.S = 75mg/L SiNPs + Fungal stress, T9 + F.S = 100mg/L SiNPs + Fungal stress, T10 = 125mg/L SiNPs + Fungal stress. Bars sharing the same letter are not significantly different at $P < 0.05$.

Discussion

Under fungal stress, the decline in relative water content (RWC) of wheat leaves observed in this study is likely attributable to pathogen-induced damage to cellular membranes, impaired root function, and disrupted water uptake, all of which adversely affect plant water status. Fungal infection can also exacerbate oxidative stress, leading to increased cellular dehydration (Wang et al., 2010). The significant improvement in leaf RWC at specific concentrations of silver (25-75 mg/L) and silica (50-100 mg/L) nano-priming suggests that the protective effects of nano-priming are dose-dependent. At optimal concentrations, nanoparticles may enhance antioxidant defense systems, stabilize cell membranes, and improve osmotic adjustment. In the case of silica, additional strengthening of cell walls may further reduce water loss and help maintain cellular turgor under stress conditions (Kumari et al., 2024). The absence of significant effects at very low or high concentrations indicates the existence of a threshold level required to elicit a physiological response. Lower concentrations may be insufficient to activate defense mechanisms, whereas higher concentrations may exert toxic effects.

Fungal stress significantly reduced the membrane stability index (MSI), indicating membrane damage likely caused by oxidative stress induced by pathogen infection. Fungal invasion typically enhances the production of reactive oxygen species (ROS), resulting in lipid peroxidation, electrolyte leakage, and loss of membrane integrity compared to healthy control plants (Hou et al., 2020; Khan et al., 2020). The observed improvement in MSI with all concentrations of silica nanoparticles and moderate doses of silver nanoparticles (50 and 75 mg/L) suggests enhanced membrane protection under stress. Silica is known to strengthen cell walls, improve structural rigidity, and reduce membrane permeability, thereby limiting pathogen penetration and electrolyte leakage. Moreover, both silica and silver nanoparticles at optimal concentrations may stimulate antioxidant enzyme systems (e.g., catalase and peroxidase), reducing ROS accumulation and protecting membrane lipids from peroxidation (Maghsoudi et al., 2016).

The significant reduction in protein content under biotic stress may be attributed to increased proteolytic activity, oxidative damage, and the diversion of

metabolic energy toward defense responses rather than protein synthesis. Pathogen infection disrupts normal cellular metabolism, leading to degradation of structural and enzymatic proteins (Rithesh et al., 2023). The highest protein content observed at 75 mg/L AgNPs suggests that an optimal concentration of silver nanoparticles enhances stress tolerance by stimulating antioxidant defense systems (Khan et al., 2020), thereby protecting the cellular machinery involved in protein synthesis. This concentration likely maintains cellular redox balance and reduces oxidative damage. Similarly, the improvement in protein content at 100 mg/L SiNPs in both stressed and non-stressed plants indicates that silica nanoparticles may enhance nitrogen metabolism, enzyme activity, and cellular structural stability. Silica is known to improve nutrient uptake and strengthen plant tissues, thereby supporting enhanced protein biosynthesis (Verma et al., 2022).

Soluble sugars play a fundamental role in cellular homeostasis and act as key organic osmolytes. In addition to their metabolic function, sugars serve as signaling molecules that interact with hormonal pathways and influence plant immune responses (Ahmad et al., 2016). Under biotic stress, plants often accumulate soluble sugars as a protective mechanism to maintain osmotic balance, provide energy, and support the synthesis of defense compounds. The observed increase in sugar content in wheat leaves may be attributed to stress signaling and enhanced metabolic activity. At higher nanoparticle concentrations (≥ 75 mg/L), additional stress signaling may stimulate greater osmolyte accumulation, thereby strengthening plant defense responses. Alternatively, increased sugar accumulation may result from improved photosynthetic efficiency, protection of chloroplast integrity, and enhanced metabolic activity induced by silver and silica nanoparticles (Nasirzadeh et al., 2022).

Under fungal stress, a reduction in leaf osmotic potential is a commonly reported response, as disease conditions disrupt normal water relations. This was consistent with the present study, where reduced RWC was observed under pathogen invasion. Fungal infection compromises membrane integrity and leads to resource reallocation toward defense mechanisms, resulting in decreased water potential in leaf tissues. This reduction reflects the accumulation of solutes (e.g., sugars and proline), as also observed in the present study. Similar responses have been documented under salinity and other stress conditions, where osmotic potential declines as part of stress adaptation, reducing cellular turgor and water balance (Naseem et al., 2023). AgNPs and SiNPs further reduced osmotic potential in both stressed and non-stressed plants in a concentration-dependent manner. These nanoparticles may alter membrane permeability and influence hormonal and antioxidant signaling pathways (Zanetti et al., 2016), thereby affecting solute accumulation and water potential. However, these effects appear to be dual in nature: while osmotic adjustment may represent a protective response, excessive nanoparticle concentrations may impose additional stress or disrupt normal cellular processes. This highlights that nanoparticle effects on osmotic potential are dose-, species-, and stress-dependent.

Silver nanoparticles at 75 mg/L resulted in the highest chlorophyll content compared to other treatments. Under biotic stress, plants often modulate chlorophyll levels as part of their adaptive response, and nanoparticles may facilitate this adjustment (Perez-Bueno et al., 2019; Javad et al., 2023). AgNPs have been reported to improve physiological processes by inhibiting fungal growth and reducing toxin production (Salama, 2012). Similarly, optimal concentrations of green-synthesized AgNPs have been shown to enhance chlorophyll and carotenoid contents in rice (Gupta et al., 2018). Chlorophyll a and b are essential pigments for photosynthesis (Motyka et al., 2020), and their reduction under pathogen stress is a common indicator of leaf senescence. Previous studies have reported decreased chlorophyll and carotenoid contents in infected plants compared to controls and nanoparticle-treated plants (Hossain et al., 1999; Barickman et al., 2014).

Proline accumulation is a typical adaptive response to both abiotic and biotic stresses. As a free amino acid, proline functions as an osmoprotectant, stabilizes proteins and membranes, and scavenges ROS, thereby maintaining cellular redox balance. The significantly higher proline content observed in stressed plants compared to controls reflects a general defense mechanism to mitigate stress-induced damage (Jaleel et al., 2008; Hayat et al., 2012; Ahmed et al., 2016). However, the reduction in proline content at specific AgNP concentrations and at all levels of SiNPs relative to stress alone suggests that these nanoparticle treatments may have alleviated stress severity. The antimicrobial properties of AgNPs (Anum et al., 2024) likely reduced pathogen load, while silica nanoparticles enhanced

structural integrity and antioxidant defenses (Verma et al., 2022). Furthermore, nanoparticles may influence nitrogen metabolism and proline biosynthesis pathways.

In the present study, biotic stress significantly increased the activities of antioxidant enzymes, including SOD, POD, and CAT, indicating activation of ROS-scavenging defense mechanisms. Fungal infection disrupts cellular redox balance, leading to the accumulation of ROS such as superoxide radicals and hydrogen peroxide, which can damage membranes, proteins, and chloroplasts (Abbasi et al., 2018). Similar increases in antioxidant enzyme activities have been reported in infected plants, where enhanced antioxidant responses are associated with improved stress tolerance and reduced oxidative damage (Farida et al., 2020; Hirpara and Gajera, 2020; Iswarya et al., 2020). Thus, the elevated antioxidant activity observed in wheat reflects an adaptive protective response against *Fusarium* head blight (FHB)-induced oxidative stress.

Nano-priming with AgNPs and SiNPs further modulated these enzymatic activities in a concentration-dependent manner. The lack of significant effects at the lowest concentrations suggests that these levels were insufficient to activate defense signaling pathways. In contrast, higher concentrations significantly enhanced antioxidant enzyme activities under both control and stressed conditions, indicating effective induction of stress-responsive mechanisms. Both nanoparticles exhibited maximum positive effects at 100 mg/L, likely due to their distinct functional roles. Silicon contributes to strengthening structural barriers and enhancing antioxidant capacity, thereby improving ROS detoxification efficiency (Alzahrani et al., 2018; Fatemi et al., 2021); while silver nanoparticles provide antimicrobial activity coupled with mild oxidative signaling that activates defense enzymes. Overall, these findings demonstrate that nano-priming at optimal doses enhances wheat tolerance to fungal stress by reinforcing the antioxidant defense system and maintaining cellular redox homeostasis (Anum et al., 2024).

Conclusion

The present study demonstrates that seed priming with green-synthesized silver and silica nanoparticles can effectively enhance physiological performance and antioxidant defense, thereby inducing resistance against *Fusarium* head blight in wheat in a dose-dependent manner. Optimal concentrations were identified as 75 mg/L for AgNPs and 100 mg/L for SiNPs, which significantly improved key attributes, including membrane stability, chlorophyll content, osmolyte accumulation, and antioxidant enzyme activities. However, higher concentrations exhibited potential toxicity, highlighting the importance of precise dose optimization for nano-priming applications. Overall, these nanoparticles effectively mitigated the adverse effects of fungal stress. Future research should focus on long-term field evaluations, environmental safety, and toxicity assessments to ensure the sustainable and practical application of nanoparticle-based technologies in agriculture.

Author's contributions

FB conducted the experiments, performed data analysis, and prepared the initial manuscript draft. SI conceived and supervised the study, guided the experimental design, and critically revised the manuscript for intellectual content. KJ and SJ critically evaluated the study, contributed to editing and refinement, and enhanced the scientific clarity and overall presentation. All authors reviewed and approved the final version of the manuscript.

Research Funding

This research did not receive any grant from funding agencies.

Conflict of Interest

The authors declare no conflict of interest.

Sustainable Development Goals Targeted

SDG 2: Zero Hunger
SDG 12: Responsible Consumption and Production
SDG 13: Climate Action

Policy Addressed

The study adhered to international biosafety and environmental guidelines, including the Cartagena Protocol, OECD nanomaterial safety recommendations, and FAO principles, alongside national regulations of Pak-EPA and the National Biosafety Committee for safe nanoparticle use.

References

Ahmad, P., Abdel Latef, A.A., Hashem, A., Abd_Allah, E.F., Gucel, S., Tran, L.S.P., 2016. Nitric oxide mitigates salt stress by regulating levels of osmolytes and antioxidant enzymes in chickpea. Frontiers in Plant Science 7, 347.

Alzahrani, Y., Kuşvuran, A., Alharby, H.F., Kuşvuran, S.,

Rady, M.M., 2018. The defensive role of silicon in wheat against stress conditions induced by drought, salinity or cadmium. Ecotoxicology and Environmental Safety 154, 187-196.

Anum, F., Jabeen, K., Javad, S., Habtemariam, S., Sharifi-Rad, J., Almarhoon, Z., Calina, D., 2024. Green synthesis of silver nanoparticles using *Amaranthus viridis*, *Mentha piperita* and *Ocimum basilicum* and their in vitro antioxidant and antifungal activity against *Botrytis cinerea*. Minerva Biotechnology and Biomolecular Research 36.

Arnon, D.I., 1949. Copper enzyme in isolated chloroplasts: polyphenoxidase in *Beta vulgaris*. Journal of Pharmaceutical Industries 24, 1-15.

Barickman, T.C., Kopsell, D.A., Sams, C.E., 2014. Abscisic acid increases carotenoid and chlorophyll concentrations in leaves and fruit of two tomato genotypes. Journal of the American Society for Horticultural Science 139, 261-266.

Barrs, H.D., Weatherly, P.E., 1962. A re-examination of relative turgidity for estimating water deficit in leaves. Australian Journal of Biological Sciences 15, 413-428.

Bates, L.S., Waldren, R.P., Teare, I.D., 1973. Rapid determination of free proline for water stress studies. Plant and Soil 39, 205-207.

Beauchamp, C., Fridovich, I., 1971. Superoxide dismutase: improved assays and an assay applicable to acrylamide gel. Analytical Biochemistry 44, 276-287.

Brady, N., 1990. Characteristics of saline and sodic soils. In The Nature and Properties of Soils, 243-246. Macmillan Publishing Company, New York.

Capell, B., Doerffling, K., 1993. Genotype-specific differences in chilling tolerance of maize in relation to chilling-induced changes in water status and abscisic acid accumulation. Physiologia Plantarum 88, 638-646.

Dubois, M., Gilles, K.A., Hamilton, J.K., Rebers, P.A., Smith, F., 1956. Colorimetric method for determination of sugars and related substances. Analytical Chemistry 28, 350-356.

Estefan, G., Sommer, R., Ryan, J., 2012. Methods of soil, plant, and water analysis: A manual for the West Asia and North Africa region, 100-105. International Center for Agricultural Research in the Dry Areas, Beirut, Lebanon.

Farida, M.S.H., Karamian, R., Albrectsen, B.R., 2020. Silver nanoparticles pollutants activate oxidative stress responses and rosmarinic acid accumulation in sage. Physiologia Plantarum 170, 514-532.

Fatemi, H., Esmaiel Pour, B., Rizwan, M., 2021. Foliar application of silicon nanoparticles affected the growth, vitamin C, flavonoid, and antioxidant enzyme activities of coriander (*Coriandrum sativum* L.) plants grown in lead-spiked soil. Environmental Science and Pollution Research 28, 1417-1425.

Gorin, N., Heidema, F.T., 1976. Peroxidase activity in Golden Delicious apples as a possible parameter of ripening and senescence. Journal of Agricultural and Food Chemistry 24, 200-201.

Goyal, A., Prasad, R., 2010. Some important fungal diseases and their impact on wheat production. In: Management of Fungal Plant Pathogens. Wallingford UK: CABI. pp. 362-373.

Gupta, S.D., Agarwal, A., Pradhan, S., 2018. Phytostimulatory effect of silver nanoparticles on rice seedling growth: an insight from antioxidative enzyme activities and gene expression patterns. Ecotoxicology and Environmental Safety 161, 624-632.

Hayat, S., Hayat, Q., Alyemeni, M.N., Wani, A.S., Pichtel, J., Ahmad, A., 2012. Role of proline under changing environments: a review. Plant Signaling and Behavior 7, 1456-1466.

Hirpara, D.G., Gajera, H.P., 2020. Green synthesis and antifungal mechanism of silver nanoparticles derived from chitin-induced exometabolites of *Trichoderma interfusant*. Applied Organometallic Chemistry 34, e5407.

Hossain, M.T., Zahangir Alam, M., Absar, N., 1999. Changes in nutrients and enzyme contents in mango leaves infected with *Colletotrichum gloeosporioides*. Indian Phytopathology 52, 75-76.

Hou, R., Shi, J., Ma, X., Wei, H., Hu, J., Tsang, Y.F., Gao, M.T., 2020. Effect of phenolic acids derived from rice straw on *Botrytis cinerea* infection in tomato. Waste and Biomass Valorization 11, 6555-6562.

Hovmøller, M.S., Walter, S., Bayles, R.A., Hubbard, A., Flath, K., Sommerfeldt, N., Leconte, M., Czembor, P., Rodriguez-Algaba, J., Thach, T., Hansen, J.G., 2016. Replacement of the European wheat yellow rust population by new races from the centre of diversity in the near-Himalayan region. Plant Pathology 65, 402-411.

Hu, C., Chen, P., Zhou, X., Li, Y., Ma, K., Li, S., Liu, H., Li, L., 2022. Arms race between the host and pathogen

associated with Fusarium head blight of wheat. Cells 11, 2275.

Hussain, S., Younas, Z., Abasi, F., Nazik, M., Ahmad, F., Raja, N.I., Mukhtar, T., Manzoor, Z., Khan, R., Mashwani, Z.U.R., 2026. Deciphering the potential of silver-selenium nanocomposites on growth metrics, physiological attributes, and antioxidant profiles in cotton (*Gossypium hirsutum* L.). Plant Nano Biology 16, 100271. https://doi.org/10.1016/j.plana.2026.100271

Iswaraya, A., Anjugam, M., Gopi, N., Shanthi, S., Govindarajan, M., Alharbi, N.S., Vaseeharan, B., 2022. β-Glucan binding protein-based silver nanoparticles enhance the wound healing potential and disease resistance in *Oreochromis mossambicus* against *Aeromonas hydrophila*. Microbial Pathogenesis 162, 105360.

Jaleel, C.A., Sankar, B., Sridharan, R., Panneerselvam, R., 2008. Soil salinity alters growth, chlorophyll content, and secondary metabolite accumulation in *Catharanthus roseus*. Turkish Journal of Biology 32, 79-88.

Jamil, Z., Mukhtar, T., Raja, M.U., Shahbaz, M., Seelan, J.S.S., Tatar, M., Ali, A., Fatima, N., Bejaoui, R., Usanmaz Bozhüyük, A., 2025. Utilization of phytogenic silver nanoparticles and bacterial agents for the management of citrus canker disease. Turkish Journal of Agriculture and Forestry 49, 998-1008.

Javad, S., Maqsood, S., Shah, A.A., Singh, A., Shah, A.N., Nawaz, M., Mosa, W.F., 2023. Iron nanoparticles mitigate cadmium toxicity in *Triticum aestivum*: modulation of antioxidative defense system and physicochemical characteristics. Journal of King Saud University Science 35, 102498.

Khan, I., Raza, M.A., Awan, S.A., Shah, G.A., Rizwan, M., Ali, B., Huang, L., 2020. Amelioration of salt-induced toxicity in pearl millet by seed priming with silver nanoparticles: oxidative damage, antioxidant enzymes, and ion uptake are major determinants of salt tolerance capacity. Plant Physiology and Biochemistry 156, 221-232.

Kumari, A., Gupta, A.K., Sharma, S., Jadon, V.S., Sharma, V., Chun, S.C., Sivanesan, I., 2024. Nanoparticles as a tool for alleviating plant stress: mechanisms, implications, and challenges. Plants 13, 1528.

Lichtenthaler, H.K., Wellburn, A.R., 1983. Determination of total carotenoids and chlorophylls a and b of leaf extracts in different solvents. Biochemical Society Transactions 11, 591-592.

Lowry, O.H., Rosebrough, N.J., Farr, A.L., Randall, R.J., 1951. Protein measurement with the Folin–phenol reagent. Journal of Biological Chemistry 193, 265-275.

Maghsoudi, K., Emam, Y., Pessarakli, M., 2016. Effect of silicon on photosynthetic gas exchange, pigments, membrane stability, and relative water content of wheat cultivars under drought stress. Journal of Plant Nutrition 39, 1001-1015.

Malhotra, S.P.K., Alghuthaymi, M.A., 2022. Biomolecule-assisted biogenic synthesis of metallic nanoparticles. In: Agri-Waste Microbial Production of Sustainable Nanomaterials, 139-163.

McDonald, B.A., Linde, C., 2002. Pathogen population genetics, evolutionary potential, and durable resistance. Annual Review of Phytopathology 40, 349-379.

McLean, E.O., 1982. Soil pH and lime requirement. In: Methods of Soil Analysis: Part 2 Chemical and Microbiological Properties 9, 199-224.

Mehak, A., Akram, A., Ali, A., Raja, N.I., Mukhtar, T., Seelan, J.S.S., Shahbaz, M., 2026. Nano-TiO_2 as a sustainable strategy to control root-knot nematodes (*Solanum lycopersicum* L.). Physiological and Molecular Plant Pathology, 103122. https://doi.org/10.1016/j.pmpp.2026.103122

Motyka, O., Štrbová, K., Zinicovscaia, I., 2020. Chlorophyll content in two medicinal plant species following nano-TiO_2 exposure. Bulletin of Environmental Contamination and Toxicology 104, 373-379.

Naseem, A., Iqbal, S., Jabeen, K., Umar, A., Alharbi, K., Antar, M., Grądecka-Jakubowska, K., Gancarz, M., Ali, I., 2023. Organic amendments improve salinity-induced osmotic and oxidative stress tolerance in okra (*Abelmoschus esculentus* (L.) Moench). BMC Plant Biology 23, 522.

Nasirzadeh, L., Kvarnheden, A., Sorkhilaleloo, B., Hervan, E.M., Fatehi, F., 2022. Foliar-applied selenium nanoparticles alleviate cadmium stress and improve yield and antioxidant capacity of wheat (*Triticum aestivum* L.). Journal of Soil Science and Plant Nutrition 22, 2469-2480.

Nazir, K., Mukhtar, T., Javed, H., 2019. In vitro effectiveness of silver nanoparticles against root-knot nematode (*Meloidogyne incognita*). Pakistan Journal of Zoology 51, 2077-2083.

Perez-Bueno, M.L., Pineda, M., Barón, M., 2019. Phenotyping plant response to biotic stress by chlorophyll fluorescence imaging. Frontiers in Plant Science 10, 477268.

Premchandra, G.S., Saneoka, H., Ogata, S., 1990. Cell membrane stability as an indicator of drought tolerance in soybean. Journal of Agricultural Science 115, 63-66.

Rayment, G.E., Higginson, F.R., 1992. Australian Laboratory Handbook of Soil and Water Chemical Methods. Inkata Press, Melbourne, 330.

Rithesh, L., Chandran, R., Deepa, John, A., 2023. Plant defence mechanisms against pathogens: structural and biochemical defence. In: Recent Trends in Agriculture 3, 227-248.

Sabir, S., Arshad, M., Ilyas, N., Naz, F., Amjad, M.S., Malik, N.Z., Chaudhari, S.K., 2022. Protective role of foliar-applied green synthesized silver nanoparticles against wheat stripe rust caused by *Puccinia striiformis*. Green Processing and Synthesis 11, 29-34.

Sairam, R.K., 1994. Effect of moisture-stress on physiological activities of two contrasting wheat genotypes. Indian Journal of Experimental Biology 32, 594-597.

Salama, H.M., 2012. Effects of silver nanoparticles on common bean (*Phaseolus vulgaris* L.) and corn (*Zea mays* L.). International Research Journal of Biotechnology 3, 190-197.

Schöneberg, T., Kibler, K., Wettstein, F.E., Bucheli, T.D., Forrer, H.R., Musa, T., Mascher, F., Bertossa, M., Keller, B., Vogelgsang, S., 2019. Influence of environmental factors on infection and mycotoxin production by *Fusarium langsethiae* and *Fusarium poae* in oats. Plant Pathology 68, 173-184.

Shahbaz, M., Akram, A., Raja, N.I., Mukhtar, T., Mehak, A., Fatima, N., Ajmal, M., Ali, K., Mustafa, N., Abasi, F., 2023. Antifungal activity of green synthesized selenium nanoparticles in mango under malformation disease. PLOS ONE 18, e0274679. https://doi.org/10.1371/journal.pone.0274679

Sujata, S., Shivam, S., Aarti, A., Rani, K., Kumar, A., 2023. Antifungal activity of green synthesized silica nanoparticles against *Phytophthora infestans*. Biochemical and Cellular Archives 24(1). 10.51470/bca.2024.24.1.1029

Sultana, K., Ahmad, B., Rauf, A., Huang, L., Ramadan, M.F., 2019. Synthesis and pharmacological activities of silver nanoparticles using plant extracts. Bioinspired, Biomimetic and Nanobiomaterials 9, 7-15.

Teranishi, Y., Tanaka, A., Osumi, M., Fukui, S., 1974. Catalase activity of hydrocarbon-utilizing *Candida* yeast. Agricultural and Biological Chemistry 38, 1213-1216.

Verma, K.K., Song, X.P., Chen, Z.L., Tian, D.D., Rajput, V.D., Singh, M., Minkina, T., Li, Y.R., 2022. Silicon and nanosilicon mitigate nutrient deficiency under stress. In: Silicon and Nano-Silicon in Environmental Stress Management and Crop Quality Improvement 1, 207-218.

Vetter, J.L., Steinberg, M.P., Nelson, A.L., 1958. Quantitative determination of peroxidase in sweet corn. Journal of Agricultural and Food Chemistry 6, 39-41.

Wang, G.P., Hui, Z., Li, F., Zhao, M.R., Zhang, J., Wang, W., 2010. Improvement of heat and drought tolerance in wheat by glycinebetaine accumulation. Plant Biotechnology Reports 4, 213-222.

Zanetti, L.V., Milanez, C.R.D., Gama, V.N., Aguilar, M.A.G., Souza, C.A.S., Campostrini, E., Ferraz, T.M., Figueiredo, F.A.M.M.D.A., 2016. Leaf application of silicon in cacao under water deficit. Pesquisa Agropecuária Brasileira 51, 215-222.